Uncertainty and sensitivity analysis for reducing greenhouse gas emissions from wastewater treatment plants

Giorgio Mannina, Alida Cosenza and Taise Ferreira Rebouças

ABSTRACT

This paper presents the sensitivity and uncertainty analysis of a plant-wide mathematical model for wastewater treatment plants (WWTPs). The mathematical model assesses direct and indirect (due to the energy consumption) greenhouse gases (GHG) emissions from a WWTP employing a whole-plant approach. The model includes: (i) the kinetic/mass-balance based model regarding nitrogen; (ii) two-step nitrification process; (iii) N_2O formation both during nitrification and denitrification (as dissolved and off-gas concentration). Important model factors have been selected by using the Extended-Fourier Amplitude Sensitivity Testing (FAST) global sensitivity analysis method. A scenario analysis has been performed in order to evaluate the uncertainty related to all selected important model factors (scenario 1), important model factors related to the influent features (scenario 2) and important model factors related to the operational conditions (scenario 3). The main objective of this paper was to analyse the key factors and sources of uncertainty at a plant-wide scale influencing the most relevant model outputs: direct and indirect (DIR,CO_{2eq} and IND,CO_{2eq}, respectively), effluent quality index (EQI), chemical oxygen demand (COD) and total nitrogen (TN) effluent concentration (COD_{OUT} and TN_{OUT}, respectively). Sensitivity analysis shows that model factors related to the influent wastewater and primary effluent COD fractionation exhibit a significant impact on direct, indirect and EQI model factors. Uncertainty analysis reveals that outflow TN_{OUT} has the highest uncertainty in terms of relative uncertainty band for scenario 1 and scenario 2. Therefore, uncertainty of influential model factors and influent fractionation factors has a relevant role on total nitrogen prediction. Results of the uncertainty analysis show that the uncertainty of model prediction decreases after fixing stoichiometric/kinetic model factors.

Key words | energy demand, greenhouse gas emission, modelling, plant-wide assessment, uncertainty

Giorgio Mannina (corresponding author)
Alida Cosenza
Taise Ferreira Rebouças
Engineering Department,
Università di Palermo,
Viale delle Scienze, 90128 Palermo,
Italy
E-mail: *giorgio.mannina@unipa.it*

Giorgio Mannina
College of Environmental Science and Engineering,
Tongji University,
1239 Siping Road, Yangpu District, Shanghai,
200092,
China

HIGHLIGHTS

- A plant-wide model for wastewater treatment plants has been applied.
- Direct and indirect greenhouse gases emissions have been investigated.
- Sensitivity and uncertainty analysis have been performed.
- Influent wastewater features strongly influence the greenhouse gases emissions.
- Uncertainty of influential model factors has a relevant role on total nitrogen prediction.

doi: 10.2166/wst.2020.231

GRAPHICAL ABSTRACT

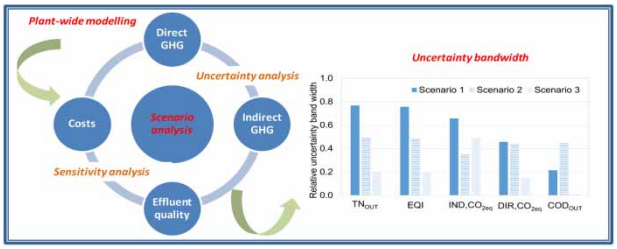

INTRODUCTION

The interest towards greenhouse gas (GHG) emissions from wastewater treatment plants (WWTPs) has considerably increased during the last decade (Kampschreur *et al.* 2009; Corominas *et al.* 2012; Mannina *et al.* 2016a). WWTPs can be a source of GHGs emissions as: direct (due to the biological processes), indirect internal (due to electric or thermal energy consumption) and indirect external (due to sludge disposal or chemicals production) emission (IPCC 2013). The waste and wastewater sector accounts for about 3% of the global GHG emissions (IPCC 2013). In order to reduce GHG emissions from WWTPs, researchers and professionals have three main aims: (i) mitigate pollutants emissions (both liquid and gaseous) (including GHGs); (ii) maintain the required quality of the treated wastewater; (iii) limit as much as possible the operational cost (Flores-Alsina *et al.* 2014; Mannina *et al.* 2016a).

In view of achieving these aims, several efforts have been provided in literature for establishing mathematical tools able to predict WWTP behaviour (in terms of GHG and liquid pollutants) (Kyung *et al.* 2015; Mannina *et al.* 2016a, 2016b, 2016c). Several modelling methods have been proposed to include GHG assessment (e.g. empirical models, process-based models often related to mass balance, dynamic mechanistic models often associated with life cycle assessment at plant wide-scale) (among others, Flores-Alsina *et al.* 2014; Bisinella de Faria *et al.* 2016; Mannina *et al.* 2017, 2018a). For each of the aforementioned modelling methods, plant-wide modelling approach can offer a straightway and effective solution for assisting in developing strategies aimed at reducing GHG emissions and improving environmental protection. Plant-wide mathematical models adopting dynamic mechanistic approaches are characterized by providing accurate predictions; however, they are more time demanding than simple comprehensive process-based models (Corominas *et al.* 2012). Therefore, despite the advantages of dynamic mechanistic models in terms of accurateness of the predictions, for a rapid GHG estimation, the simple comprehensive process-based models are suggested (Mannina *et al.* 2016a). However, it has to be mentioned that simple comprehensive process-based models are often based on a great number of assumptions and their response can be highly uncertain. Therefore, uncertainty analysis may help in obtaining model confidence and improve the model predictions. However, sensitivity and uncertainty analysis have rarely been performed in the GHG WWTP modelling studies with the aim to identify the key source of uncertainty (Behera *et al.* 2020). The existing studies mainly consider only the water line treatment (such as Mannina *et al.* 2017). Sweetapple *et al.* (2013) have performed an uncertainty analysis of a GHG plant-wide model, however they adopted a dynamic mechanistic modelling approach. Further, Mannina *et al.* (2016b, 2016c) have performed an uncertainty analysis of a GHG plant-wide comprehensive process-based model but without considering all the possible N_2O emissions pathways.

Bearing in mind the above introduction, in this study, sensitivity and uncertainty analysis of a new simple processes-based model have been performed in view of identifying the key sources of uncertainty.

MATERIALS AND METHODS

Mathematical model and case study

The model adopted here is based on chemical oxygen demand (COD), total suspended solids (TSS) mass-balance and nitrogen kinetic/mass-balance. The model consists of 29 model factors (divided into kinetic, stoichiometric,

Table 1 | Symbol, description, unit, value at T = 20 °C, variation range and reference for each model factor

Symbol	Description	Unit	Value T = 20 °C	Min	Max	Reference
SRT_{ASP}	Sludge retention time of the activated sludge process section	day	10	6	18	Metcalf & Eddy (2003)
r_{NO}	Internal recycle rate from aerobic to anoxic reactor	–	4	2	5	Metcalf & Eddy (2003)
OTE	Oxygen transfer efficiency	%	15	0.09	0.18	Metcalf & Eddy (2003)
μ	Maximum growth rate of heterotrophic biomass	d^{-1}	5.985	4	8	Hauduc *et al.* (2011)
k_s	Half saturation parameter for heterotrophic biomass	gCOD m^{-3}	15	14	21	Hauduc *et al.* (2011)
k_d	Decay rate for heterotrophic biomass	d – 1	0.825	0.5	1.5	Hauduc *et al.* (2011)
Y_H	Yield for heterotrophic biomass growth	gVSS gCOD – 1	0.565	0.38	0.75	Hauduc *et al.* (2011)
$iNVSS_{PS}$	N content of biomass in the primary sludge	kgN kgVSS – 1	0.085785	0.0665	0.13	Brun *et al.* (2002), Gori *et al.* (2011)
$iNVSS_{SS}$	N content of biomass in the secondary sludge	kgN $kgVSS^{-1}$	0.1197	0.0665	0.13	Brun *et al.* (2002), Gori *et al.* (2011)
$\mu_{N,AOB}$	Maximum growth rate of autotrophic biomass	d^{-1}	0.078	0.0546	0.1014	Hauduc *et al.* (2011)
$K_{N,AOB}$	Half saturation parameter for autotrophic biomass	gNH_4-N m^{-3}	1	0.7	1.3	Hauduc *et al.* (2011)
$k_{dN,AOB}$	Decay rate for autotrophic biomass	d^{-1}	0.096	0.0672	0.1248	Hauduc *et al.* (2011)
$Y_{N,AOB}$	Yield of autotrophic biomass growth	gVSS gNH_4-N	0.18	0.126	0.234	Brun *et al.* (2002)
$\mu_{N,NOB}$	Maximum growth rate for autotrophic NOB biomass	gVSS $gVSS^{-1}day^{-1}$	0.78	0.546	1.014	Pocquet *et al.* (2016)
$K_{N,NOB}$	Half-saturation parameter for autotrophic NOB biomass	gNH_4-N m^{-3}	1	0.7	1.3	Pocquet *et al.* (2016)
$k_{dN,NOB}$	Decay rate of autotrophic NOB biomass	gVSS $gVSS^{-1}day^{-1}$	0.096	0.0672	0.1248	Pocquet *et al.* (2016)
$Y_{N,NOB}$	Yield for autotrophic NOB biomass growth	gVSS gNH_4-N^{-1}	0.06	0.042	0.078	Pocquet *et al.* (2016)
pCOD/VSS	Ratio between particulate COD and volatile suspended solids	–	1.466325	1.07	1.87	Gori *et al.* (2011)
$nbsCOD_{IN}$	Fraction of soluble nonbiodegradable COD in influent wastewater	–	0.033915	0.034	0.12	Mannina *et al.* (2011), Gori *et al.* (2011)
$pbCOD_{IN}$	Fraction of particulate biodegradable COD in influent wastewater	–	0.4478775	0.1	0.45	Mannina *et al.* (2011), Gori *et al.* (2011)
$npbCOD_{IN}$	Fraction of particulate nonbiodegradable COD in influent wastewater	–	0.245385	0.05	0.25	Mannina *et al.* (2011), Gori *et al.* (2011)
$nbsCOD_{PI}$	Fraction of soluble nonbiodegradable COD in the primary effluent	–	0.069825	0.034	0.12	Mannina *et al.* (2011), Gori *et al.* (2011)
$pbCOD_{PI}$	Fraction of particulate biodegradable COD in the primary effluent	–	0.3082275	0.1	0.45	Mannina *et al.* (2011), Gori *et al.* (2011)
$npbCOD_{PI}$	Fraction of particulate nonbiodegradable COD in the primary effluent	–	0.13566	0.05	0.25	Mannina *et al.* (2011), Gori *et al.* (2011)
SRT_{DIG}	Sludge retention time of the anaerobic digestion	day	20	16	28	Metcalf & Eddy (2003)
$K_{d,dig}$	Decay rate for biomass during digestion	d^{-1}	0.06	0.02	0.08	Cakir and Stenstrom (2005)
$Y_{H,dig}$	Yield for heterotrophic biomass growth during digestion	gVSS gCOD	0.0225	0.01	0.03	Cakir and Stenstrom (2005)
EF_{CO2}	CO_2 emission factor due to the headworks	gCO_2 L^{-1}	0.00448875	0.00405	0.00495	Czeplel *et al.* (1993)
EF_{CH4}	CH_4 emission factor due to the headworks	gCO_{2eq} L^{-1}	0.00013965	0.000126	0.000154	Czeplel *et al.* (1993)

Table 2 | Summary of the model state variables; the state variables in bold have been here introduced

Symbol	Unit	Description
$mCO_{2,HD}$	kg_{CO2eq}/day	Emission of CO_2 at the headworks (HD)
$mCO_2eq,CH_{4,HD}$	kg_{CO2eq}/day	Equivalent CO_2 emission of CH_4 at the HD
$mCO_{2,ASP}$	kg_{CO2eq}/day	Emission of CO_2 due to biomass respiration at the activated sludge process (ASP)
$mCO_2eq,CH_{4,ASP}$	kg_{CO2eq}/day	Equivalent CO_2 emission of CH_4 at the ASP
$mCO_2eq,N_2O,_{ASP,AOB}$	kg_{CO2eq}/day	Equivalent CO_2 emission of N_2O due to AOB biomass respiration
$mCO_2eq,N_2O,_{ASP,DEN}$	kg_{CO2eq}/day	Equivalent CO_2 emission of N_2O due to heterotrophic biomass respiration
$mCO_{2,AD}$	kg_{CO2eq}/day	Emission of CO_2 during anaerobic digestion (AD)
$mCO_2,CH_4,comb,BG$	kg_{CO2eq}/day	Emission of CO_2 due to biogas (BG) combustion (comb)
$mCO_2eq,CH_{4,AD}$	kg_{CO2eq}/day	Equivalent CO_2 due to CH_4 emissions during sludge digestion at the AD
$mCO_2eq,CH_4fugitive,_{AD}$	kg_{CO2eq}/day	Equivalent CO_2 due to CH_4 fugitive emissions during AD
$mCO_2eq,CH_{4,D}$	kg_{CO2eq}/day	Equivalent CO_2 due to CH_4 emissions during dewatering (D)
$mCO_2eq,_{TB}$	kg_{CO2eq}/day	Equivalent CO_2 emitted due to biosolid discharge (TB)
$mCO_2eq,N_2O,_{EFF}$	kg_{CO2eq}/day	Equivalent CO_2 emitted due to effluent discharge (EFF)
$mCO_2eq,offset$	kg_{CO2eq}/day	Equivalent CO_2 credit due to energy recovery (e_R)
$e_{D,HD}$	kWh/day	Energy demand in HD units
$e_{D,PS}$	kWh/day	Energy demand in PS unit
$e_{D,ASP}$	kWh/day	Energy demand in ASP units
$e_{D,SS}$	kWh/day	Energy demand in SS unit
$e_{D,AD}$	kWh/day	Energy demand in AD unit
$e_{D,D}$	kWh/day	Energy demand in dewatering unit
e_R	kWh/day	Energy recovery

influent fractionation and operational factors) and 21 state variables. Tables 1 and 2 summarize the detailed description of model factors and state variables, respectively. The model allows to assess the total equivalent CO_2 (CO_{2eq}) emissions ($kgCO_{2,eq}$/day or $kgCO_{2,eq}$/treated volume) from a WWTP as the sum between direct (DIR,CO_{2eq}) and indirect (IND,CO_{2eq}) emissions. The model considers uniform and constant influent features over time. Further, non-biodegradable compounds are considered conservative.

The model adopted here introduces the following main innovative aspects related to up-to-date available literature plant-wide models: (i) kinetic/mass-balance based model regarding nitrogen; (ii) includes the nitrification as a two-step process; (iii) includes the N_2O formation during nitrification and denitrification both in dissolved and off-gas forms. More specifically, the autotrophic biomass is divided into autotrophic ammonia oxidizing bacteria (AOB) and nitrite oxidizing biomass (NOB) in view of modelling the N_2O formation processes during nitrification. The secondary effluent ammonia and nitrite concentration are calculated according to the mass balance analysis of a well-mixed activated sludge reactor (Metcalf & Eddy 2003). Thus, the effluent ammonia concentration depends on the AOB kinetics parameters and on the sludge retention time. The dissolved N_2O concentration inside the aerobic reactor is modelled according to the relationship proposed by Wu *et al.* (2014), while the dissolved and gaseous N_2O concentration inside and from the anoxic reactor is modelled according to the relationships proposed by and Yan *et al.* (2017). According to Yan *et al.* (2017) the gaseous N_2O emitted from the anoxic reactor depends on the carbon to nitrogen ratio. The model allows to assess DIR,CO_{2eq} and IND,CO_{2eq} emissions at a plant-wide scale, considering the contribution due to the water line (headworks (HD), primary settler (PS), activated sludge process (ASP), secondary settler (SS), treated effluent discharge (EFF)) and to the sludge line (anaerobic digestion (AD), dewatering (D), biosolids disposal (TB) and energy recovery (ER) due to the biogas combustion) (Figure 1).

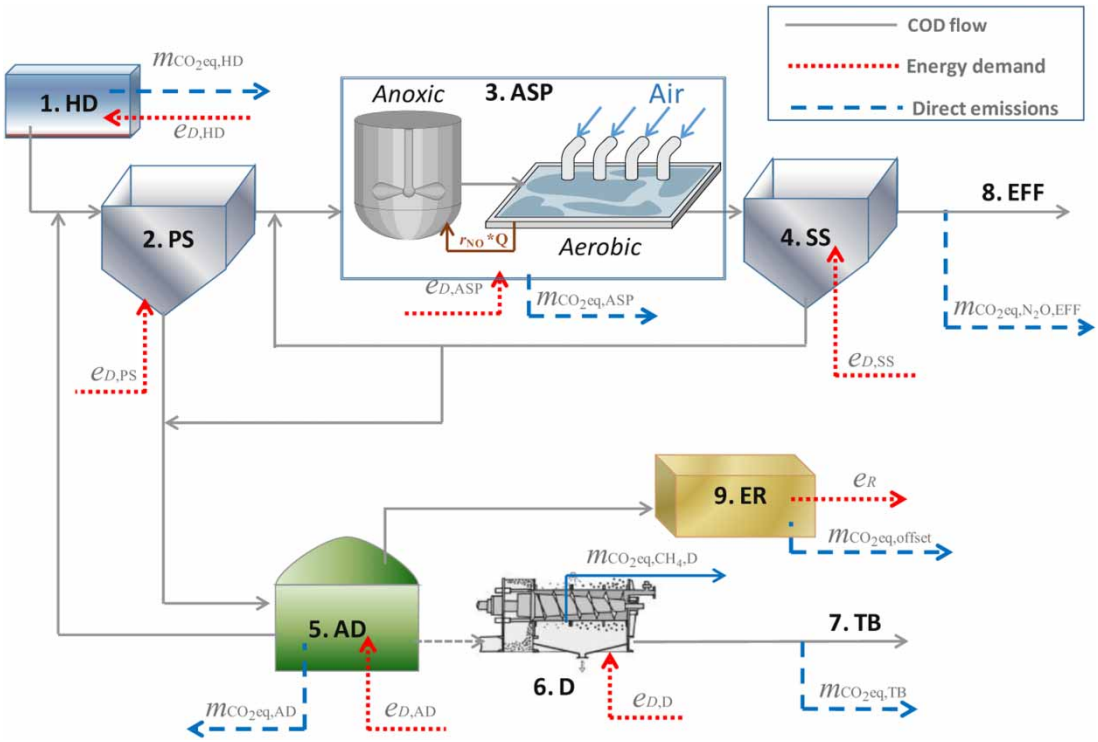

Figure 1 | Layout of the plant under study: HD = headworks; PS = primary settler; ASP = activated sludge process; SS = secondary settler; AD = anaerobic digester; D = sludge dewatering; TB = biosolids disposal; EFF = treated effluent; ER = energy recovery; the meaning of symbols is detailed in Tables 1 and 2.

The DIR,CO_{2eq} and IND,CO_{2eq} have been calculated according to Equations (1) and (2), respectively (the meaning of symbols is reported in Table 2).

$$DIR, CO_{2eq} = m_{CO2eq,HD} + m_{CO2eq,ASP} + m_{CO2eq,AD} + m_{CO2,CH4comb,BG} + m_{CO2eq,CH4,D} + m_{CO2eq,TB} + m_{CO2eq,N2O,EFF} - m_{CO2eq,offset} \quad (1)$$

The term $m_{CO2eq,ASP}$ includes all the direct and equivalent CO_2 emissions from the activated sludge process: due to biomass respiration ($m_{CO2,ASP}$), due to CH_4 ($m_{CO2eq,CH4,ASP}$) and due to AOB ($m_{CO2eq,N2O,ASP,AOB}$) and NOB ($m_{CO2eq,N2O,ASP,NOB}$) respiration.

$$IND, CO_{2eq} = (e_{D,HD} + e_{D,PS} + e_{D,ASP} + e_{D,SS} + e_{D,AD} + e_{D,D} - e_R) \cdot sEnCO_{2,eq} \quad (2)$$

In this study, the value of the specific CO_2 equivalent emission for energy consumption ($SEnCO_{2,eq}$) suggested by EIA (2009) has been adopted; the sum in brackets of Equation (3) represents the total energy demand of the plant (e_D).

Energy recovery (e_R, kW/day) is calculated as presented in Equation (3) by multiplying the biogas production (m_{BG}, kg/day) by the efficiency of the energy recovery (η_{eR}) and by methane specific energy (h_{BG}, kW/kgBG).

$$e_R = m_{BG}\eta_{eR}h_{BG} \quad (3)$$

The model has been applied to a conventional activated sludge (CAS) WWTP having the Ludzack-Ettinger (anoxic and aerobic biological reactors) configuration for nitrogen removal (Figure 1). The plant treats 60,000 $m^3\ d^{-1}$ of real wastewater and consists of a water line (headworks, primary settler, CAS units according to Ludzack-Ettinger configuration, secondary settler and disinfection unit) and a sludge line (anaerobic sludge digester with energy recovery, sludge dewatering unit) (Mannina *et al.* 2016b, 2016c) (Figure 1). A detailed description of the model can be found in Mannina *et al.* (2019, 2020).

Sensitivity analysis method

Sensitivity analysis has been performed by using the Extended-FAST method (Saltelli *et al.* 2004). This method belongs to the global sensitivity analysis methods and is

based on the variance decomposition theorem. Two sensitivity indices for each i-th model factor have been calculated: the first-order effect index (S_i) and the total-effect index (S_{Ti}). S_i quantifies the contribution of the i-th model factor to the variance of the model output [Var(Y)] without considering the interaction among the model factors; it is expressed as:

$$S_i = \frac{Var_{xi}(E_{x_{-i}}(Y|X_i))}{Var(Y)} \quad (4)$$

where E is the expectancy operator and Var is the variance. The subscripts indicate that the operation is either applied 'over the i-th factor' x_i, or 'over all model factors except the i-th model factor' x-i (Saltelli *et al.* 2004).

S_{Ti} is expressed as:

$$S_{Ti} = 1 - \frac{Var_{x-i}(E_{x_i}(Y|X_{-i}))}{Var(Y)} \quad (5)$$

The difference between S_{Ti} and S_i represents the interaction among the model factors. The Extended-FAST method requires nxNR simulations, where n is the number of factors and NR is the number of runs per model factor (NR = 500–1,000 according to Saltelli *et al.* 2004).

Uncertainty analysis and scenario analysis

The uncertainty analysis has been performed by running Monte Carlo simulations varying the model factors selected as important through the GSA. More specifically, three uncertainty scenarios have been investigated by Monte Carlo simulations changing the following factors: scenario 1 – all model important factors; scenario 2 – model factors related to the influent features; scenario 3 – model factors related to the operational conditions.

For each scenario, results of the Monte Carlo simulations have been interpreted by analysing the cumulative distribution function (CDF). Specifically, for each model output, the CDF of the normalized value has been considered; the normalized value has been obtained by dividing each simulated value by the maximum one. Moreover, the comparison of the uncertainty analysis results among the model outputs taken into account for each scenario has been performed by comparing the value of the relative uncertainty bandwidth. This latter has been computed by dividing the width between the 5th and 95th percentiles for the 50th percentile.

Simulation conditions and numerical settings

Sensitivity analysis has been performed by considering all model factors (influent fractionation factors, kinetic factors, conversion factors and emission factors) and five model outputs (see Table 2). Specifically, the following model outputs have been considered: DIR, CO_{2eq}, IND, CO_{2eq}, the total effluent COD and nitrogen concentration (COD_{OUT} and TN_{OUT}) and the effluent quality index (EQI). The EQI, expressed in kg pollution unit per day [kgPU day^{-1}], has been calculated according to Equation (6).

$$EQI = \frac{1}{T \cdot 1000} \int_{t0}^{t1} (\beta_{COD} \cdot COD_{OUT} + \beta_{TN} \cdot TN_{,OUT}) \cdot Q_{OUT} dt \quad (6)$$

where β_{COD} and β_{TN} are, respectively, the weighted factors of the effluent COD (COD_{OUT}) and TN (TN_{OUT}), Q_{OUT} is the flow rate of treated wastewater and T represents the reference time.

TN_{OUT} includes non-oxidized ammonia, nitrite, nitrate and dissolved nitrous oxide while organic nitrogen is neglected. β_{COD} and β_{TN} have been considered equal to 1 and 20, respectively, according to literature (Maere *et al.* 2011).

For a detailed description of the symbol and variation range of each factor the reader is referred to Table 1. Due to the lack of knowledge about the distribution of the model factors, a uniform prior distribution was considered for each factor. The Extended-FAST method was applied using the sensitivity package developed by Pujol (2007) in the R environment (Development Core Team, 2007). For the Extended-FAST application, 1,000 NR have been considered, consequently 29,000 simulations have been run.

To classify important, non-influential and interacting factors, thresholds of the sensitivity measures were selected. Specifically, factors with S_i value greater than 0.01, at least for one model output, were classified as important. Interacting model factors were selected using the normalised index value (S_{Ni}), which corresponds to the ratio between the interaction of the i-th model factor related to one model output and the maximum value among the interactions for that model output. Factors with S_{Ni} greater than 0.5 for at least one model output were considered to be interacting. Model factors with S_{Ni} and S_i values lower than 0.5 and 0.01, respectively, were considered to be non-influential. The uncertainty analysis was performed by all the model

factors classified as important or interacting. For each analysed scenario, 1,000 Monte Carlo simulations (by adopting a Latin Hypercube Sampling) have been performed.

RESULTS AND DISCUSSION

Sensitivity analysis

In Figure 2, the Extended-FAST results for each analysed model output are reported. For sake of shortness, the values of S_i, S_{Ti}, S_{Ti}-S_i and S_{Ni} are summarized in Table 3.

The sum of S_i explains more than 94% of the total variance for all model outputs suggesting that the model is highly linear and additive. This statement is also confirmed by the value of the sum of S_{Ti}, which is always close to 1. This latter result suggests that a very low interaction among factors takes place. By applying the Extended-FAST method, 17 model factors resulted to be important (S_i > 0.01 and/or S_{Ni} > 0.5) for at least one model output.

By analyzing data reported in Figure 2, one can observe that six factors have significant impact on DIR,$CO_{2,eq}$. Specifically, $npbCOD_{IN}$, pCOD/VSS, $nbsCOD_{IN}$, $pbCOD_{IN}$, $pbCOD_{PI}$ and $npbCOD_{PI}$ (S_i equal to 0.78, 0.064, 0.051, 0.081, 0.011 and 0.011, respectively) have an S_i value higher than 0.01 for DIR,$CO_{2,eq}$. Among these factors, three ($npbCOD_{IN}$, $nbsCOD_{IN}$, and $pbCOD_{IN}$) are related to the influent wastewater fractionation, two ($pbCOD_{PI}$ and $npbCOD_{PI}$) are related to the primary effluent fractionation and one (pCOD/VSS) refers to particulate COD and volatile suspended solids.

Influent fractionation factors are also strongly interacting; indeed, the S_{Ni} value for $npbCOD_{IN}$ and $pbCOD_{IN}$ is equal to 1 and 0.67, respectively (Figure 2, Table 3). The influent fractionation factors influence the bCOD availability to heterotrophic biomass growth and, consequently, the direct CO_2 produced during the biomass respiration value.

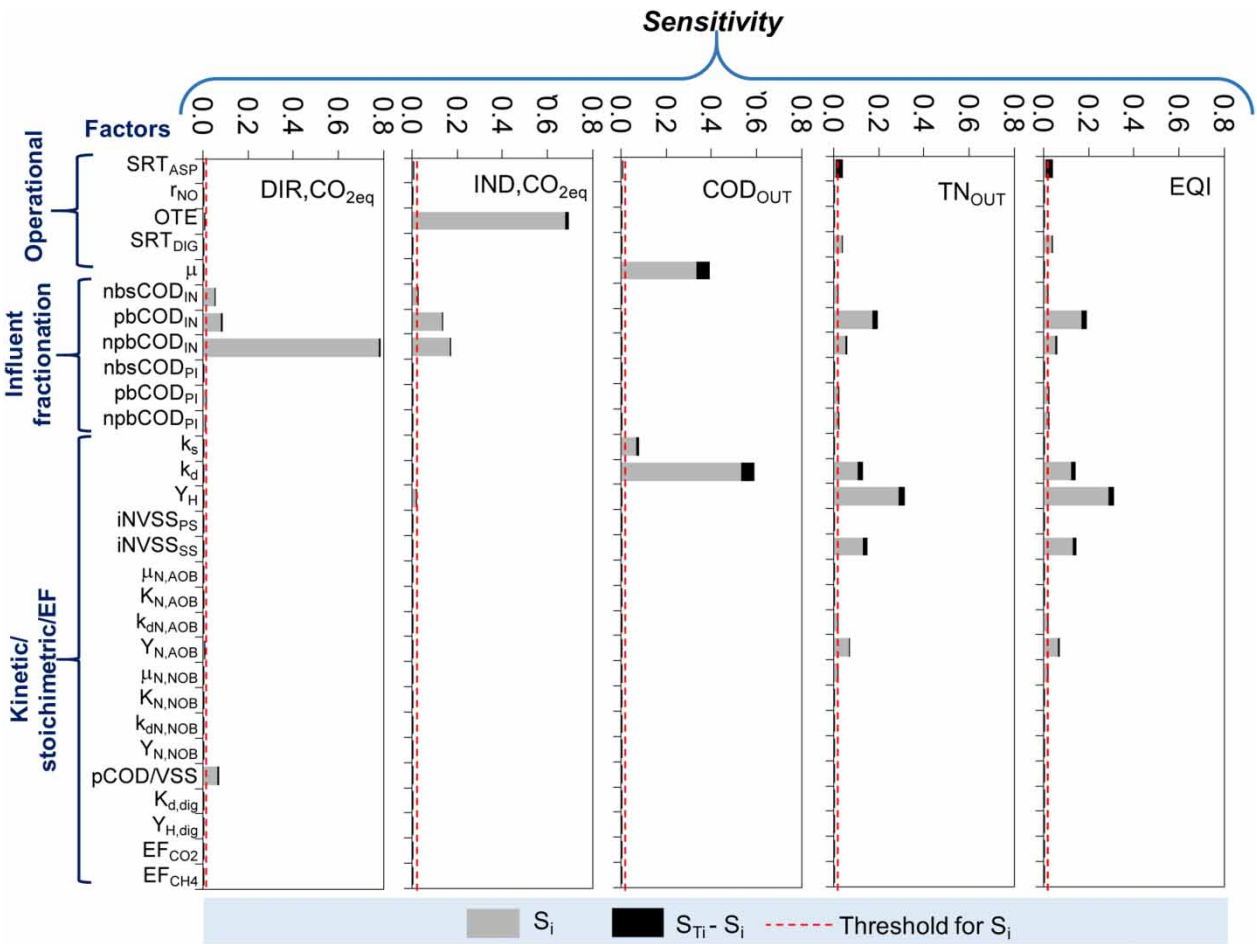

Figure 2 | Sensitivity (S_i), interaction ($S_{Ti} - S_i$) and threshold values of all model factors, with the five model output taken into account.

For example, the higher the $nbsCOD_{IN}$ fraction and the lower the availability of substrate to be degraded during the biomass metabolism (both during aerobic and anoxic conditions). Hence, CO_2 produced during the biomass respiration is reduced as a result of the conservative nature of $nbsCOD_{IN}$. Further, even the physical processes occurring inside the primary settler (as demonstrated by the importance of $pbCOD_{PI}$ and $npbCOD_{PI}$) can influence the COD availability for the biomass respiration and consequently the $DIR,CO_{2,eq}$.

The indirect emissions ($IND,CO_{2,eq}$) are mostly influenced by three main factors: the oxygen transfer efficiency (OTE) (S_i equal to 0.679), fractionation factors ($nbsCOD_{IN}$, $pbCOD_{IN}$ and $npbCOD_{IN}$ with S_i equal to 0.024, 0.132 and 0.167, respectively) and the yield coefficient for heterotrophic biomass growth (Y_H) (S_i equal to 0.015 (Figure 2, Table 3). Such results are consistent with literature which shows that energy consumption is mostly due to the activate sludge process (ASP): More specifically, ASP consumes are in the range of 60–70% (Mamais *et al.* 2015; Mannina *et al.* 2018b; Massara *et al.* 2018).

OTE is an important factor for the indirect emissions since regulates the air flow rate required to maintain the aerobic conditions inside the aerobic reactor. Similarly, $nbsCOD_{IN}$, $pbCOD_{IN}$ and $npbCOD_{IN}$ are important factors for indirect emissions since they regulate the availability of soluble COD required for the biological processes. For example, as the fraction of sCOD decreases the oxygen required for the aerobic processes decreases, thus influencing the power requirements of the aeration process and of the entire WWTP. Finally, the yield coefficient (Y_H) influences the amount of the air flow to be inserted in the aerobic reactor and consequently the power requirements.

The COD_{OUT} is mostly influenced by the maximum growth rate of heterotrophic biomass (μ), the half-saturation factor for heterotrophic biomass (k_s, S_i equal to 0.067) and the decay rate of heterotrophic biomass (k_d, S_i equal to 0.532). Among these factors μ and k_d also resulted to be interacting having an S_{Ni} value of 1 and 0.98, respectively. All model factors resulted to be important for COD_{OUT} have a key role on regulating the heterotrophic active biomass inside the aerobic reactor, thus influencing the COD consumption and consequently the COD concentration in the effluent wastewater.

Eleven model factors mostly related to the influent fractionation, heterotrophic, AOB and NOB resulted to be important for the total nitrogen at the effluent (TN_{OUT}) (Figure 2, Table 3). Among these factors, it is important to observe that Y_H (S_i equal to 0.289), which is directly related to the heterotrophic biomass, is the most important factor for TN_{OUT} (with an S_i value equal to 0.29). This result is related to the anoxic activity of heterotrophic biomass which strongly influences the amount of nitrogen removed from the system and consequently the TN_{OUT}. Conversely, the model interacting factor for TN_{OUT} is the sludge retention time of the conventional activated process (SRT_{ASP}) (S_i and S_{Ni} value equal to 0.01 and 1, respectively). Indeed, SRT_{ASP} is a key factor for different processes occurring inside the system. Among these processes, SRT_{ASP} also regulates the autotrophic biomass growth within the aerobic reactor (nitrification). The nitrification process is responsible for the nitrate availability to be denitrified and consequently removed from the system.

Finally, the EQI is influenced by 13 model factors. Among these factors, five are related to the influent COD fractionation ($nbsCOD_{IN}$, $pbCOD_{IN}$, $npbCOD_{IN}$, $pbCOD_{PI}$ and $npbCOD_{PI}$), five to the biomass activity (k_d, Y_H, $k_{dN,AOB}$, $Y_{N,AOB}$ and $\mu_{N,NOB}$), one to the nitrogen content in the secondary sludge ($iNVSS_{SS}$) and two to the operational conditions (SRT_{DIG}, SRT_{ASP}) (Figure 2, Table 3). Among these factors, Y_H has the highest S_i value (0.28), indicating that the role of heterotrophic bacteria is relevant in terms of pollutants discharge (both nitrogen and COD) (Figure 2, Table 3), while the influence of SRT_{ASP} is only due to the interaction contribution. Indeed, despite the value of S_i for SRT_{ASP} (related to EQI) being lower than 0.01, this factor proved to be important due its high interaction. Indeed, the S_{TI}-S_i and S_{Ni} value resulted to be equal to 0.03 and 1, respectively. The high interaction of SRT_{ASP} is mainly due to the complexity of the model in terms of biological processes which are strongly regulated by SRT_{ASP}.

Uncertainty analysis

The uncertainty analysis was performed by considering the three scenarios described earlier. For each scenario, Monte Carlo simulations have been performed by varying important model factors grouped according to the scenarios.

In Figure 3, the cumulative distribution functions (CDFs) of $DIR,CO_{2,eq}$, $IND,CO_{2,eq}$, EQI, COD_{OUT} and TN_{OUT} of each scenario is reported.

In Figure 3, x-axes report the normalized value of each model output. The normalized value has been obtained by dividing each Monte Carlo output model value by the maximum one. From a visual inspection of Figure 3, one may observe that the width of the uncertainty bands, (calculated as difference between the 95th and 5th percentiles of the

Table 3 | Symbol, S_i, S_{Ti}, S_{Ti}-S_i and S_{Ni} values for each model factors and model output

	EQI				DIR,CO_{2eq}				IND,CO_{2eq}				COD_{OUT}				TN_{OUT}			
Factors	**S_i**	**S_{Ti}**	**S_{Ti}-S_i**	**S_{Ni}**	**S_i**	**S_{Ti}**	**S_{Ti}-S_i**	**S_{Ni}**	**S_i**	**S_{Ti}**	**S_{Ti}-S_i**	**S_{Ni}**	**S_i**	**S_{Ti}**	**S_{Ti}-S_i**	**S_{Ni}**	**S_i**	**S_{Ti}**	**S_{Ti}-S_i**	**S_{Ni}**
SRT_{ASP}	0.010	0.039	0.029	**1.000**	0.001	0.002	0.001	0.103	0.006	0.008	0.002	0.109	0.006	0.007	0.001	0.019	**0.010**	0.040	0.030	**1.000**
r_{NO}	0.000	0.002	0.002	0.084	0.000	0.000	0.000	0.040	0.000	0.000	0.000	0.006	0.000	0.000	0.000	0.003	0.000	0.002	0.002	0.083
OTE	0.000	0.002	0.002	0.084	0.005	0.006	0.001	0.120	**0.679**	0.694	0.015	**1.000**	0.000	0.000	0.000	0.003	0.000	0.002	0.002	0.083
SRT_{DIG}	**0.036**	0.040	0.003	0.110	0.000	0.001	0.000	0.059	0.000	0.000	0.000	0.007	0.000	0.000	0.000	0.002	**0.037**	0.041	0.003	0.110
μ	0.001	0.003	0.002	0.085	0.000	0.001	0.001	0.065	0.000	0.000	0.000	0.014	**0.336**	0.394	0.058	**1.000**	0.000	0.003	0.002	0.083
$nbsCOD_{IN}$	**0.015**	0.020	0.004	0.149	**0.051**	0.052	0.000	0.054	**0.024**	0.025	0.001	0.076	0.000	0.000	0.000	0.002	**0.015**	0.020	0.004	0.147
$pbCOD_{IN}$	**0.168**	0.192	0.024	**0.813**	**0.080**	0.085	0.005	**0.674**	**0.132**	0.139	0.007	0.480	0.000	0.000	0.000	0.002	**0.171**	0.195	0.024	**0.811**
$npbCOD_{IN}$	**0.050**	0.060	0.010	0.343	**0.780**	0.787	0.008	**1.000**	**0.167**	0.173	0.006	0.422	0.000	0.000	0.000	0.002	**0.051**	0.061	0.010	0.343
$nbsCOD_{PI}$	0.000	0.003	0.003	0.090	0.000	0.000	0.000	0.048	0.000	0.000	0.000	0.007	0.000	0.000	0.000	0.002	0.000	0.003	0.003	0.090
$pbCOD_{PI}$	**0.020**	0.023	0.003	0.107	**0.011**	0.012	0.001	0.137	0.001	0.001	0.000	0.008	0.000	0.000	0.000	0.002	**0.020**	0.023	0.003	0.107
$npbCOD_{PI}$	**0.022**	0.025	0.003	0.105	**0.011**	0.012	0.001	0.119	0.001	0.001	0.000	0.007	0.000	0.000	0.000	0.002	**0.022**	0.026	0.003	0.105
k_s	0.000	0.003	0.002	0.086	0.000	0.001	0.000	0.058	0.000	0.000	0.000	0.012	**0.067**	0.079	0.012	0.210	0.000	0.003	0.002	0.084
k_d	**0.120**	0.141	0.021	**0.723**	0.000	0.001	0.001	0.082	0.002	0.003	0.001	0.052	**0.532**	0.589	0.057	**0.979**	**0.107**	0.128	0.020	**0.690**
Y_H	**0.287**	0.313	0.026	**0.896**	0.000	0.001	0.001	0.104	**0.015**	0.017	0.002	0.131	0.000	0.000	0.000	0.002	**0.289**	0.315	0.026	**0.885**
$iNVSS_{PS}$	0.000	0.003	0.003	0.118	0.000	0.000	0.000	0.062	0.000	0.000	0.000	0.014	0.000	0.000	0.000	0.002	0.000	0.003	0.003	0.117
$iNVSS_{SS}$	**0.129**	0.146	0.017	**0.593**	0.001	0.001	0.001	0.084	0.000	0.000	0.000	0.015	0.000	0.000	0.000	0.002	**0.131**	0.148	0.017	**0.588**
$\mu_{N,AOB}$	0.000	0.002	0.002	0.083	0.000	0.000	0.000	0.034	0.000	0.000	0.000	0.007	0.000	0.000	0.000	0.002	0.000	0.002	0.002	0.082
$K_{N,AOB}$	0.000	0.002	0.002	0.063	0.000	0.000	0.000	0.027	0.000	0.000	0.000	0.006	0.000	0.000	0.000	0.002	0.000	0.002	0.002	0.062
$k_{dN,AOB}$	**0.017**	0.020	0.003	0.106	0.001	0.001	0.000	0.044	0.000	0.000	0.000	0.005	0.000	0.000	0.000	0.002	**0.017**	0.020	0.003	0.105
$Y_{N,AOB}$	**0.065**	0.071	0.005	0.187	0.004	0.005	0.001	0.077	0.000	0.000	0.000	0.005	0.000	0.000	0.000	0.002	**0.066**	0.071	0.005	0.185
$\mu_{N,NOB}$	**0.016**	0.022	0.005	0.189	0.001	0.002	0.000	0.060	0.000	0.000	0.000	0.007	0.000	0.000	0.000	0.002	**0.017**	0.022	0.006	0.186
$K_{N,NOB}$	0.000	0.001	0.001	0.040	0.000	0.000	0.000	0.017	0.000	0.000	0.000	0.005	0.000	0.000	0.000	0.002	0.000	0.001	0.001	0.040
$k_{dN,NOB}$	0.000	0.004	0.004	0.147	0.000	0.000	0.000	0.046	0.000	0.000	0.000	0.007	0.000	0.000	0.000	0.002	0.000	0.004	0.004	0.145
$Y_{N,NOB}$	0.000	0.003	0.003	0.105	0.000	0.000	0.000	0.030	0.000	0.000	0.000	0.005	0.000	0.000	0.000	0.002	0.000	0.003	0.003	0.103
pCOD/VSS	0.000	0.003	0.003	0.105	**0.064**	0.070	0.007	**0.888**	0.002	0.003	0.000	0.026	0.000	0.000	0.000	0.002	0.000	0.003	0.003	0.103
$K_{d,dig}$	0.000	0.003	0.003	0.087	0.000	0.000	0.000	0.055	0.000	0.000	0.000	0.007	0.000	0.000	0.000	0.002	0.000	0.003	0.003	0.087
$Y_{H,dig}$	0.000	0.003	0.003	0.087	0.000	0.000	0.000	0.055	0.000	0.000	0.000	0.007	0.000	0.000	0.000	0.002	0.000	0.003	0.003	0.087
EF_{CO2}	0.000	0.003	0.003	0.087	0.000	0.000	0.000	0.054	0.000	0.000	0.000	0.007	0.000	0.000	0.000	0.002	0.000	0.003	0.003	0.087
EF_{CH4}	0.000	0.003	0.003	0.087	0.000	0.000	0.000	0.054	0.000	0.000	0.000	0.007	0.000	0.000	0.000	0.002	0.000	0.003	0.003	0.087
$\sum S$	0.96	1.15	–	–	1.01	1.04	–	–	1.03	1.07	–	–	0.94	1.07	–	–	0.96	1.15	–	–

Factors selected as important on the basis of S_i and S_{Ni} are in bold.

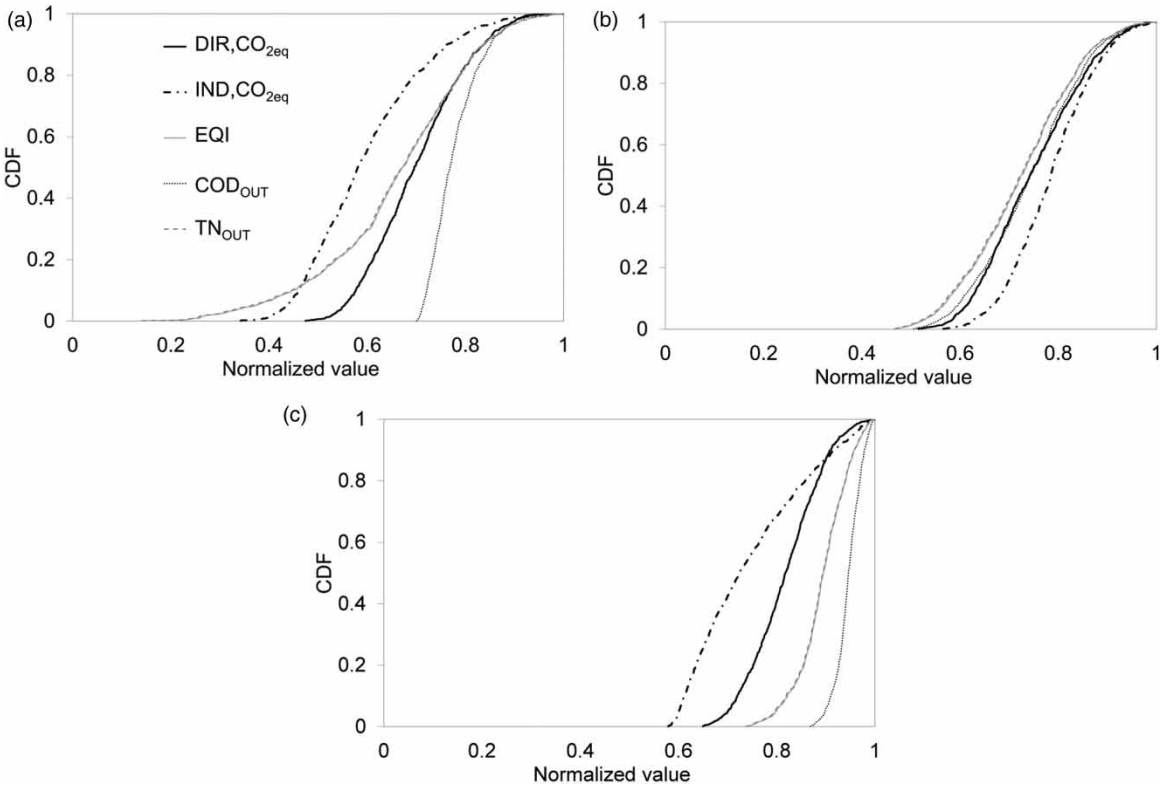

Figure 3 | Cumulative distribution function (CDF) of DIR,$CO_{2,eq}$, IND,$CO_{2,eq}$, EQI, COD_{OUT} and TN_{OUT} for scenario 1 (a), scenario 2 (b) and scenario 3 (c).

normalized values), changes with the model output and the analysed scenarios. This is mainly due to the fact that some of the model outputs entail a different level of complexity in terms of involved phenomena.

For scenario 1, where all important model factors have been varied, the uncertainty bands' widths of EQI (0.51), TN_{OUT} (0.51) and IND,$CO_{2,eq}$ (0.38) is higher than that of COD_{OUT} (0.16) and DIR,$CO_{2,eq}$ (0.32) (Figure 3(a)). This result is due to the fact that a greater number of processes influences EQI, TN and IND,$CO_{2,eq}$ than the other model output. Therefore, the uncertainty of model factors varied during Monte Carlo simulations (operational, influent fractionation and kinetic/stoichimetric factors) strongly influence the EQI, TN and IND,$CO_{2,eq}$ predictions. Conversely for scenario 2, the uncertainty band widths of TN_{OUT} (0.36), EQI (0.35), and COD_{OUT} (0.33) are higher than that of DIR,$CO_{2,eq}$ (0.32) and IND,$CO_{2,eq}$ (0.28) (Figure 3(b)). This result is mainly due to the fact that influent fractionation factors, as reported above, strongly influence TN_{OUT}, EQI and COD_{OUT}. Finally, for scenario 3, where only the influential factors related to the operational conditions were varied, the uncertainty bands' widths of IND,$CO_{2,eq}$ (0.36) and DIR,$CO_{2,eq}$ (0.24) are higher than that of EQI (0.18), TN_{OUT} (0.18), and COD_{OUT} (0.09) (Figure 3(c)). This result has relevant interest since underlines that the operational conditions may have an important role influencing both direct and indirect emissions predictions.

The results of Figure 3 show that the uncertainty band width decrease from scenario 1 to scenario 3, underlying that the reduction of the number of model factors varied from scenario 1 to scenario 3 reduce the uncertainty of model predictions. However, it is interesting to observe that from scenario 1 to scenario 2 the uncertainty bands width related to COD_{OUT} increases. This result is mainly due to the fact that the uncertainty of the influent fractionation factors, varied during in scenario 2, strongly influence the uncertainty of COD_{OUT}. Further, from scenario 2 to scenario 3, the uncertainty bands' width related to IND,$CO_{2,eq}$ increases. Such a fact underlines the key role of operational conditions in influencing the IND,$CO_{2,eq}$ predictions.

In order to provide a quantitative assessment of the model uncertainty and to make comparable the results among the model outputs, the relative uncertainty band width for each model output and scenario has been

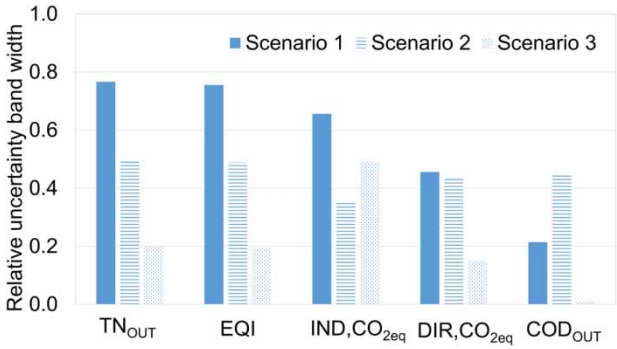

Figure 4 | Relative uncertainty bandwidth for each model output.

computed by dividing the width between the 5th and 95th percentiles to the 50th percentile. In Figure 4, the relative uncertainty band widths for each model output and scenario are reported.

By analysing Figure 4, one may observe that for scenarios 1 and 2, the highest uncertainty is related to TN due to the treated effluent (the relative uncertainty bandwidth is equal to 0.79 for scenario 1 and 0.48 for scenario 2), while for scenario 3 the highest uncertainty is related to IND,CO_{2eq} (0.47), thus, corroborating again that operational conditions mostly influence indirect emissions (scenario 3). The highest uncertainty of TN for scenarios 1 and 2 is mainly due to the uncertainty of kinetic, stoichiometric and fractionation factors which influence the biological processes and consequently the amount of nitrogen removed.

Data in Figure 4 also show a reduction of the total relative uncertainty from scenario 1 to scenario 3, therefore the uncertainty of model prediction decreases after fixing stoichimetric/kinetic model factors. This result suggest that an accurate estimation of stoichimetric/kinetic model factors has to be performed before applying the model.

CONCLUSIONS

The key findings of this study are summarised as follows:

- The sensitivity analysis reveals that model factors related to the influent wastewater and primary effluent COD fractionation exhibit a significant impact on direct, indirect and EQI model factors.
- The effluent concentration of COD and total nitrogen is mainly influenced by the heterotrophic stoichiometric/kinetic factors; revealing that for TN the role of denitrification (anoxic growth of heterotrophic bacteria) is relevant.
- The uncertainty analysis reveals that TN_{OUT} has the highest uncertainty in terms of relative uncertainty band for scenario 1 and scenario 2, thus revealing that uncertainty of all influential model factors and of influent fractionation factors has a relevant role on the total nitrogen prediction.
- Results of the uncertainty analysis show that the uncertainty of model prediction decreases after fixing stoichimetric/kinetic model factors.

REFERENCES

Behera, C. R., Al, R., Gernaey, K. V. & Sin, G. 2020 A process synthesis tool for WWTP – an application to design sustainable energy recovery facilities. *Chemical Engineering Research and Design* **156**, 353–370.

Bisinella de Faria, A. B., Ahmadi, A., Tiruta-Barna, L. & Spérandio, M. 2016 Feasibility of rigorous multi-objective optimization of wastewater management and treatment plants. *Chemical Engineering Research and Design* **115**, 394–406.

Brun, R., Kühni, M., Siegrist, H., Guejer, W. & Reichert, P. 2002 Practical identifiability of ASM2d parameters-systematic selection and tuning of parameter subsets. *Water Research* **36**, 4113–4127.

Cakir, F. Y. & Stenstrom, M. K. 2005 Greenhouse gas production: A comparison between aerobic and anaerobic wastewater treatment technology. *Water Research* **39**, 4197–4203.

Corominas, L., Flores-Alsina, X., Snip, L. & Vanrolleghem, P. A. 2012 Comparison of different modeling approaches to better evaluate greenhouse gas emissions from whole wastewater treatment plants. *Biotechnology and Bioengineering* **109** (11), 2854–2863.

Czepiel, P., Crill, P. C. & Harriss, R. C. 1993 Methane emissions from municipal wastewater treatment processes. *Environmental Science & Technology* **27** (12), 2472–2477.

Development Core Team 2007 Sensitivity: Sensitivity Analysis, R package version 1.3-0.

EIA – United States Energy Information Administration 2009 Annual Energy Outlook 2009e With projections to 2030 DOE/EIA-0383(2009), Washington, DC, USA.

Flores-Alsina, X., Arnell, M., Amerlinck, Y., Corominas, L., Gernaey, K. V., Guo, L., Lindblom, E., Nopens, I., Porro, J., Shaw, A., Snip, L., Vanrolleghem, P. A. & Jeppsson, U. 2014 Balancing effluent quality, economic cost and greenhouse gas emissions during the evaluation of (plant-wide) control/operational strategies in WWTPs. *Science of the Total Environment* **466–467**, 616–624.

Hauduc, H., Rieger, L., Takács, I., Héduit, A., Vanrolleghem, P. A. & Gillot, S. 2011 A systematic approach for model verification: application on seven published activated sludge models. *Water Science and Technology* **61** (4), 825–839.

Gori, R., Jiang, L.-M., Sobhani, R. & Rosso, D. 2011 Effects of soluble and particulate substrate on the carbon and energy footprint of wastewater treatment processes. *Water Research* **45**, 5858–5872.

IPCC, Climate Change 2013 *The Physical Science Basis. Contribution of Working Group I to the Fifth Assessment Report of the Intergovernmental Panel on Climate Change. 2013*. Cambridge University Press, Cambridge, UK and New York, NY, USA, p. 1535.

Kampschreur, M. J., Temmink, H., Kleerebezem, R., Jettena, M. S. M. & van Loosdrecht, M. C. M. 2009 Nitrous oxide emission during wastewater treatment. *Water Research* **43**, 4093–4103.

Kyung, D., Kim, M., Chang, J. & Lee, W. 2015 Estimation of greenhouse gas emissions from a hybrid wastewater treatment plant. *Journal of Cleaner Production* **95**, 117–123.

Maere, T., Verrecht, B., Moerenhout, S., Judd, S. & Nopens, I. 2011 BSM-MBR: a benchmark simulation model to compare control and operational strategies for membrane bioreactors. *Water Research* **45**, 2181–2190.

Mamais, D., Noutsopoulos, C., Dimopoulou, A., Stasinakis, A. & Lekkas, T. 2015 Wastewater treatment process impact on energy savings and greenhouse gas emissions. *Water Science and Technology* **71**, 303–308.

Mannina, G., Cosenza, A., Vanrolleghem, P. A. & Viviani, G. 2011 A practical protocol for calibration of nutrient removal wastewater treatment models. *Journal of Hydroinformatics* **13**, 575–595.

Mannina, G., Ekama, G., Caniani, D., Cosenza, A., Esposito, G., Gori, R., Garrido-Baserba, M., Rosso, D. & Olsson, G. 2016a Greenhouse gases from wastewater treatment – A review of modelling tools. *Science of the Total Environment* **551–552**, 254–270.

Mannina, G., Cosenza, A., Gori, R., Garrido-Baserba, M., Sobhani, R. & Rosso, D. 2016b Greenhouse gas emissions from wastewater treatment plants on a plantwide scale: sensitivity and uncertainty analysis. *Journal of Environmental Engineering – ASCE* **142** (6), 1. Article number 04016017.

Mannina, G., Capodici, M., Cosenza, A., Di Trapani, D. & Viviani, G. 2016c Sequential batch membrane bio-reactor for wastewater treatment: the effect of increased salinity. *Bioresource Technology* **209**, 205–212.

Mannina, G., Cosenza, A. & Ekama, G. A. 2017 Greenhouse gases from membrane bioreactors: mathematical modelling, sensitivity and uncertainty analysis. *Bioresource Technology* **239**, 353–367.

Mannina, G., Cosenza, A. & Ekama, G. A. 2018a A comprehensive integrated membrane bioreactor model for greenhouse gas emissions. *Chemical Engineering Journal* **334**, 1563–1572.

Mannina, G., Cosenza, A. & Ekama, G. 2018b Mathematical modelling of greenhouse gas emissions from membrane bioreactors: A comprehensive comparison of two mathematical models. *Bioresource Technology* **268**, 107–115.

Mannina, G., Ferreira Rebouças, T., Cosenza, A. & Chandran, K. 2019 A model for accounting carbon and energy footprint of wastewater treatment plants: model application and scenario analysis. *Cleaner Production Journal* **217**, 244–256.

Mannina, G., Ferreira Rebouças, T., Cosenza, A. & Chandran, K. 2020 A plant-wide modelling comparison between membrane bioreactors and conventional activated sludge. *Bioresource Technology* **297**, 122401.

Massara, T. M., Solís, B., Guisasola, A., Katsou, E. & Baeza, J. A. 2018 Development of an ASM2d-N_2O model to describe nitrous oxide emissions in municipal WWTPs under dynamic conditions. *Chemical Engineering Journal* **335**, 185–196.

Metcalf & Eddy, Inc. 2003 *Wastewater Engineering: Treatment and Reuse* (4th edn, G. Tchobanoglous, F. L. Burton & H. D. Stensel, eds). McGraw-Hill Series in Civil and Environmental Engineering, New York, NY, USA.

Pocquet, M., Wu, Z., Queinnec, I. & Spérandio, M. 2016 A two pathway model for N_2O emissions by ammonium oxidizing bacteria supported by the NO/N_2O variation. *Water Research* **88**, 948–959.

Pujol, G. 2007 Sensitivity: Sensitivity Analysis, R package version 1.3-0.

Saltelli, A., Tarantola, S., Campolongo, F. & Ratto, M. 2004 *Sensitivity Analysis in Practice. A Guide to Assessing Scientific Models*. Probability and Statistics Series. John Wiley & Sons Publishers, Chichester, UK.

Sweetapple, C., Fu, G. & Butler, D. 2013 Identifying key sources of uncertainty in the modelling of greenhouse gas emissions from wastewater treatment. *Water Research* **47**, 4652–4665.

Wu, G., Zheng, D. & Xing, L. 2014 Nitritation and N_2O emission in a denitrification and nitrification two-sludge system treating high ammonium containing wastewater. *Water* **6**, 2978–2992.

Yan, X., Zheng, J., Han, Y., Liu, J. & Sun, J. 2017 Effect of influent C/N ratio on N_2O emissions from anaerobic/anoxic/oxic biological nitrogen removal processes. *Environ. Sci. Pollut. Control Ser.* **24**, 23714–23724.

First received 21 October 2019; accepted in revised form 1 May 2020. Available online 15 May 2020